

Article

Color Glass by Layered Nitride Films for Building Integrated Photovoltaic (BIPV) System

Akpeko Gasonoo ¹, Hyeon-Sik Ahn ² , Seongmin Lim ², Jae-Hyun Lee ^{3,*}  and Yoonseuk Choi ^{2,*} ¹ Research Institute of Printed Electronics & 3D Printing, Industry University Cooperation Foundation, Hanbat National University, Daejeon 34158, Korea; amoebatheo2009@gmail.com² Department of Electronic Engineering, Hanbat National University, Daejeon 34158, Korea; princass123@naver.com (H.-S.A.); seongmin625@naver.com (S.L.)³ Department of Creative Convergence Engineering, Hanbat National University, Daejeon 34158, Korea

* Correspondence: jhyunlee@hanbat.ac.kr (J.-H.L.); ychoi@hanbat.ac.kr (Y.C.); Tel.: +82-42-821-1970 (J.-H.L.); +82-42-821-1134 (Y.C.)

Abstract: We investigated layered titanium nitride (TiN) and aluminum nitride (AlN) for color glasses in building integrated photovoltaic (BIPV) systems. AlN and TiN are among suitable and cost-effective optical materials to be used as thin multilayer films, owing to the significant difference in their refractive index. To fabricate the structure, we used radio frequency magnetron deposition method to achieve the target thickness uniformly. A simple, fast, and cheap fabrication method is achieved by depositing the multilayer films in a single sputtering chamber. It is demonstrated that a multilayer stack that allows light to be transmitted from a low refractive index layer to a high refractive index layer or vice-versa can effectively create various distinct color reflections for different film thicknesses and multilayer structures. It is investigated from simulation based on wave optics that TiN/AlN multilayer offers better color design freedom and a cheaper fabrication process as compared to AlN/TiN multilayer films. Blue, green, and yellow color glasses with optical transmittance of more than 80% was achieved by indium tin oxide (ITO)-coated glass/TiN/AlN multilayer films. This technology exhibits good potential in commercial BIPV system applications.

Keywords: BIPV; color glass; thin film interference; optical path-length difference; RF sputtering; nitride; multilayer film



Citation: Gasonoo, A.; Ahn, H.-S.; Lim, S.; Lee, J.-H.; Choi, Y. Color Glass by Layered Nitride Films for Building Integrated Photovoltaic (BIPV) System. *Crystals* **2021**, *11*, 281. <https://doi.org/10.3390/cryst11030281>

Academic Editors: Van-Chuc Nguyen and Ji-Hoon Lee

Received: 5 February 2021

Accepted: 10 March 2021

Published: 12 March 2021

Publisher's Note: MDPI stays neutral with regard to jurisdictional claims in published maps and institutional affiliations.



Copyright: © 2021 by the authors. Licensee MDPI, Basel, Switzerland. This article is an open access article distributed under the terms and conditions of the Creative Commons Attribution (CC BY) license (<https://creativecommons.org/licenses/by/4.0/>).

1. Introduction

The building integrated photovoltaic (BIPV) system provides a novel and an efficient technique for solar energy to be harvested from the envelope of buildings and to generate renewable energy mainly for the constructed environment [1,2]. Photovoltaics (PVs) have attracted much research interest and were established several decades ago [3,4]. Recently, the introduction of organic photovoltaics—the technology to convert sunlight into electricity by employing thin films of organic semiconductors—has been the subject of active research and has received increased interest in recent years by the industrial sector [5,6]. This technology has the potential to birth a new generation of low-cost, solar-powered products with thin and flexible form factors. BIPV concepts, which are based on PVs, are a prime way to reach net-zero energy buildings. Large-scale application and integration of solar energy technologies has enabled the general adoption and extension of distributed energy generation in buildings of all size and use across the world. This way, a significant portion of the electricity generated is consumed within the built environment, reducing the cost of electricity generation, transport, and distribution by smart grids [7].

Though BIPV systems are primarily attached to buildings to generate electricity, their general adoption as integrated solar energy system and functional materials for the building envelope is mainly hindered by aesthetic considerations. Conventional solar systems installed on large areas of buildings (roofs and facades) come in standard black or

grey solar modules, mostly due to the antireflective coating layers within the PV cell [8]. This is generally not well accepted by most users. An approach to solving this problem is adopting front color glasses that can hide the active components of the PV cell but transmits the non-reflected radiation entirely to the absorber with little or no absorption and can withstand degradation over time [9,10]. When such color glasses replace the conventional front glasses of both PV and thermal solar panels, architectural integration of solar panels into glazed building facades becomes an attractive choice.

While the choice of color is good for architecture, the colored appearance should not cause excessive energy loss and instability. Various concepts have been proposed for optical applications in color glasses for BIPV systems. Some conventional approaches adopt pigment-based coloring, which, however, absorbs radiation and does not withstand degradation over time [11]. Recently, some solutions have adopted optical color films based on interference effect from thin multilayer films [12–15]. The color is derived based on the interference in the reflected light from the different interfaces of the thin multilayer film [16–19]. The incident light undergoes reflection and refraction at every interface where multiple rays are reflected into the air, while others are transmitted through the film. The reflected rays interfere with each other, their phase difference being determined by their optical path difference (OPD) [19–21]. The degree of constructive or destructive interference between the reflected waves depends on the difference in their phases. The OPD depends on the thickness, the refractive index, and the angle of incidence of the original wave on the film. Normally, a phase shift of 180° (π radians) may be introduced upon reflection at a boundary depending on the refractive indices of the materials on either side of the boundary [19].

Kromatix™ technology [13] applied multilayer coating on the inner glass surface by atomic layer deposition in a low-pressure plasma process. Atomic layer deposition is considered to have a great potential for producing thin, uniform, and conformal films with accurate thickness control at less substrate damage [22]. However, its major limitation is slow growth rate; hence, it is expensive to be considered for large area commercial applications in BIPV systems. Typical growth rate of inorganic films by atomic layer deposition is below $2 \text{ \AA}/\text{cycle}$ [22], which is significantly low as compared to the high film growth rate of more than $60 \text{ nm}/\text{min}$ that can be achieved by magnetron sputtering [23]. Unfortunately, most of the materials selected for the multilayer structures have low refractive indices [14,24,25]. Consequently, thick layers are required to achieve bright and desired colors. This approach is expensive, requires long deposition time, and yields layers with low transmittance and cannot be applied in BIPV systems. Moreover, the effect of the structure on the optical properties of the multilayer has been elusive and must be fully investigated. Most often, the composites of the multilayer layer films are concealed from commercial applications.

Recently, we reported color glasses for BIPV systems using multilayer thin films composed of metal oxide layers [14,15]. We verified through computer simulation based on wave optics that metal oxide thin layers with significant difference in their refractive index could be integrated to realize different colors with good transmittance. Several reports have also investigated that commercially available nitrides and other dielectrics can be applied in passivation applications for advanced transparent flexible organic light emitting diodes and other organic electronic devices [23]. So far, most of the investigations have only focused on optical transparency of the dielectrics used in passivation applications. For advance and cheap PVs, it is only novel to adopt color films that can double as passivation films.

In this paper, we investigated color glass for a BIPV system using multilayer thin films composed of titanium nitride (TiN) and aluminum nitride (AlN) layers. TiN and AlN are chosen based on the significant difference in the refractive index of TiN and AlN. This material selection rule provides a multilayer that significantly changes the OPD of the reflected and transmitted spectra when the layer thickness is adjusted. To achieve high film growth rate, the TiN and AlN layers were deposited by radio frequency reactive sputtering at room temperature. Aesthetically considerable blue, green, and yellow color

glasses were fabricated from the derivatives of the glass/ITO/TiN/AlN multilayer structure. A uniform color glass with high transmittance more than 80% is demonstrated. The TiN and AlN multilayer and the proposed deposition technique provide a simple, fast, and cheap fabrication method to make color glasses that are applicable for BIPV systems.

2. Materials and Methods

The schematic structures of the multilayers used are shown in Figure 1. Figure 1a–c show the schematic structures used for simulation, while Figure 1d,e are the schematic structures used in the experiment. For the given incident light on the thin films, there are reflected rays produced at each boundary whose OPDs depend on thickness and refractive index of the layers and the angle of incidence.

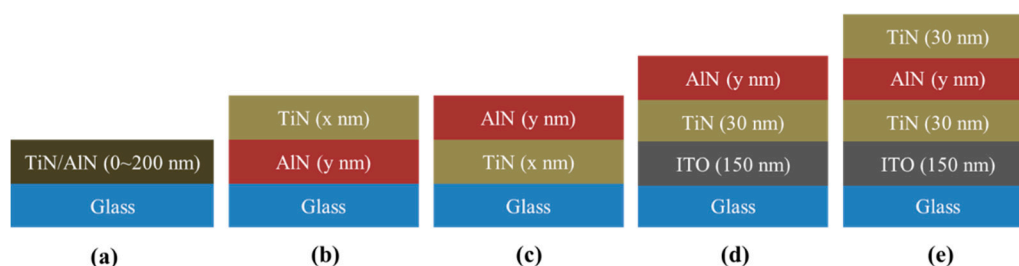


Figure 1. Schematic structure of (a) glass/titanium nitride (TiN) (0~200 nm) and glass/aluminum nitride (AlN) (0~200 nm), (b) multilayer A (glass/AlN (y nm)/TiN (x nm)), (c) multilayer B (glass/TiN (x nm)/AlN (y nm)), (d) M1 (glass/indium tin oxide (ITO) (150 nm)/TiN (30 nm)/AlN (30 nm)) and M2 (glass/ITO (150 nm)/TiN (30 nm)/AlN (50 nm)), (e) M3 (glass/ITO (150 nm)/TiN (30 nm)/AlN (30 nm)/TiN (30 nm)), and M4 (glass/ITO (150 nm)/TiN (30 nm)/AlN (50 nm)/TiN (30 nm)).

In collaboration with EMBODYTECH Inc., South Korea, a homemade radio frequency magnetron sputter was used for the deposition of the nitride films. Targets of 100 mm diameter comprising 99.999% aluminum and titanium were purchased from Sigma-Aldrich and iTASCO, respectively. Argon (Ar) and nitrogen (N_2) gases were nominally 99.999% pure. All materials were used as received. Unpatterned ITO (150 nm) glass substrates (2.5×2.5 cm) were used to fabricate the color glasses after cleaning sequentially with acetone and isopropyl alcohol in an ultrasonic bath, boiled in isopropyl alcohol, and dried in an oven at 150 °C for 15 min, respectively. TiN and AlN layers were deposited by a reactive sputtering system using the commercial aluminum and titanium targets, respectively, in a high-vacuum base pressure of 2.4 mTorr. The nitride depositions were carried out in plasma created from Ar and N_2 gas mixtures by varying the partial pressures of gases with a mass flow controller (TN2900, Nextron, Daejeon, Korea). The controlled plasma was formed adjacent to the substrate by a 300 W radio frequency energy applied using an RF power generator. The plasma dissociates the entering process gases into ions and radicals that will be deposited onto the substrate surface. A working pressure of 20 mTorr was maintained during sputtering. Pre-sputtering was conducted for about 30 min to remove oxygen from chamber and stabilize the plasma state.

Thin-film optical simulation based on wave optics was done using the Essential Macleod software program by Thin Film Center Inc. The optical transmittance and reflectance of the films were measured by ultraviolet visible near-infrared spectrophotometry (Lambda 950 UV-vis-NIR spectrophotometer, PerkinElmer, Waltham, MA, USA). The thickness of the TiN and AlN films were determined from alpha step measurements.

3. Results and Discussion

3.1. Simulation and Analysis

The simulation analysis was made based on the refractive index of the materials provided in the database of Essential Macleod software. The reported refractive index of AlN, TiN, ITO, and glass within visible range is shown in Figure 2. The refractive index at

510 nm for glass, ITO, TiN, and AlN is 1.5, 2.1, 1.2, and 2.1, respectively. The nitrides exhibit a refractive index difference of 0.9 at 510 nm, which is suitable for thin film multilayer interference. Generally, AlN exhibits similar refractive index characteristics with ITO, while that of TiN is lower than glass, especially for incident beams with wavelengths between 450 and 700 nm.

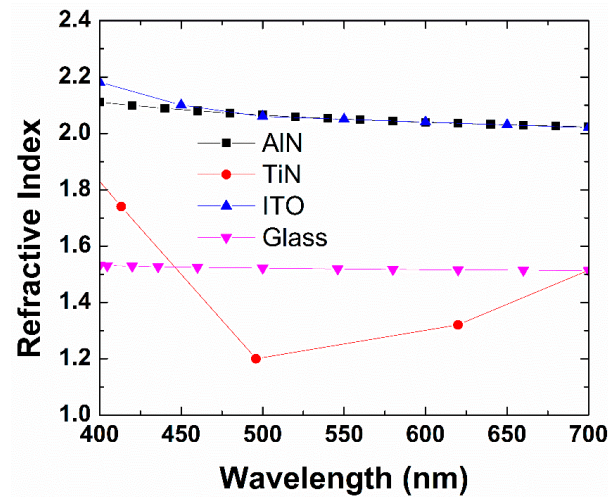


Figure 2. Refractive index of AlN, TiN, ITO, and glass.

Optimized layer thicknesses of the TiN and AlN were determined from simulation based on the schematic structure shown in Figure 1a. The thickness of each layer was varied from 0 to 200 nm. The 3D simulation profile of the reflectance as a function of thickness and wavelength in glass/TiN and glass/AlN structures are shown in Figure 3, respectively. In the case of the glass/TiN profile shown in Figure 3a, an increase in the TiN thickness to 50 nm increased reflectance to 23%. For wavelengths below 500 nm, the reflectance remains below 20% for layers more than 50 nm. However, for other wavelengths above 500 nm, the reflectance increases steadily. In the case of the glass/AlN profile shown in Figure 3b, the reflectance of AlN increased to 23% at 50 nm, decreased to 4% at 100 nm, increased back to 23% at 180 nm, and then decreased to 4.2% at 200 nm in that sequence. The above characteristics demonstrate that the reflectance and transmittance characteristics of multilayer films composed of TiN and AlN can be uniquely tuned by the thickness of the layers and the incident beams.

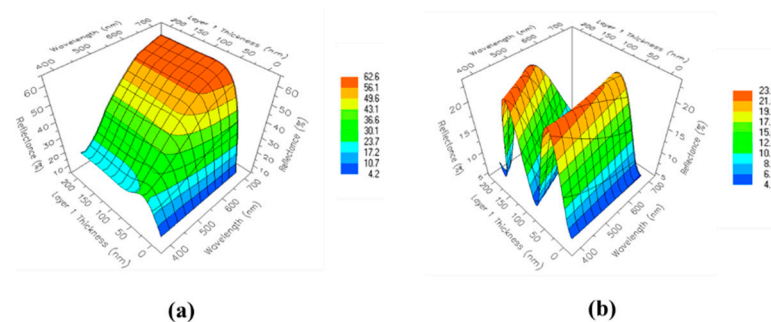


Figure 3. Simulation of reflectance profile of (a) glass/TiN and (b) glass/AlN.

The effect of the multilayer structure on the thin film interference using computer simulation based on wave optics is further investigated. Glass/AlN/TiN and glass/TiN/AlN multilayers, herein referred to as Multilayer A and Multilayer B, respectively, have been investigated. The schematic structures of Multilayer A and Multilayer B are shown in Figure 1b,c respectively. For Multilayer A, light traverses air, through to the TiN layer. Since the refractive index of TiN is higher than air, the reflection that occurs at the air–TiN boundary of the film introduces a 180° phase shift in the reflected wave [19–21]. Part of the

beam is then transmitted through the AlN layer and is similarly reflected with a phase shift. Similar interferences occur at the AlN–glass and glass–air boundaries. However, there is no phase shift in the reflected light at the AlN–glass boundary, since the beam travels from a medium with a higher refractive index into a medium with a lower refractive index. In Multilayer B, reflections occur for some wavelengths at the air–AlN, AlN–TiN, TiN–glass, and glass–air interfaces, respectively. The remaining light is transmitted sequentially through a series of alternating layers with low and high refractive index, respectively. Thus, the optical path traversed by the transmitted beam differs in the two multilayer structures. The reflected waves, which are generated at each interface within the multilayer, interact and produce a resultant reflected light wave. The intensity of the net reflected light depends on the optical thickness of the film. By varying the optical path via the thickness control and structure of the multilayer, the peaks in the reflectance or the transmittance spectra can be shifted to achieve a desired color film [19–21]. The simulated color profiles for Multilayer A and Multilayer B are shown in Figure 4, respectively.

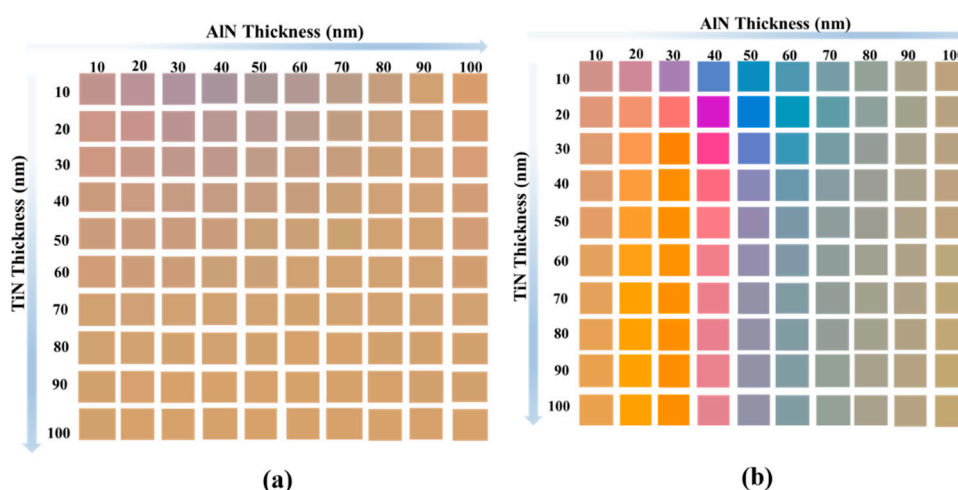


Figure 4. Simulated color profile of (a) Multilayer A and (b) Multilayer B.

The color profile for Multilayer A is shown in Figure 4a. Generally, it is shown that it is difficult to achieve various colors, even when thick layers of TiN and AlN are deposited. In cases where thick layers are deposited, the overall fabrication becomes expensive and requires a long processing time. It is most preferred to have freedom of color choice for commercial application in BIPV. Therefore, from the perspective of large-scale commercial optical applications, Multilayer A is not suitable. Figure 4b shows the simulated color profile for Multilayer B. It is demonstrated that various bright color films can be achieved, especially for layers deposited below 50 nm. This can be attributed to different OPD obtained by Multilayer B when the thickness of the layers is tuned. For each incident beam, a unique constructive interference for different film thicknesses is achieved. Thus, from the perspective of commercial application, Multilayer B provides one of the best methods for achieving color glasses, as cost and processing time are minimized as compared to the other reported approaches. Thus, our fabricated color films are based on Multilayer B. Color glasses of choice can be easily fabricated by tuning the thickness of the layers.

3.2. Samples Analysis

The TiN layer has a refractive index lower than glass, which makes it difficult to achieve several color films with glass/TiN/AlN. As such, for lab scale fabrication and demonstration, ITO-coated glass substrates were used. Four color glass derivatives of Multilayer B, herein referred to as M1, M2, M3, and M4, were fabricated based on ITO-coated glass/TiN (30 nm)/AlN (30 nm), ITO-coated glass/TiN (30 nm)/AlN (50 nm), ITO-coated glass/TiN (30 nm)/AlN (30 nm)/TiN (30 nm), and ITO-coated glass/TiN (30 nm)/AlN (50 nm)/TiN (30 nm) multilayers, respectively. The schematic structure of

M1 and M2 are shown in Figure 1d, while that of M3 and M4 are shown in Figure 1e, respectively. The actual photographs of the fabricated M1, M2, M3, and M4 color glasses are shown in Figure 5. The photographs of the samples were taken on two backgrounds, black surface and solar cell, respectively.

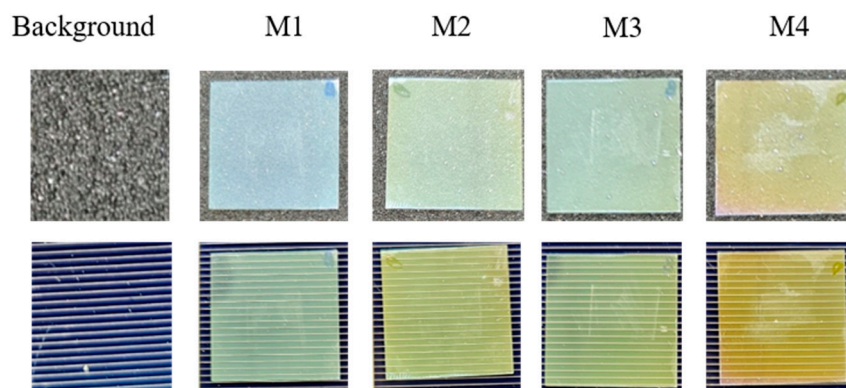


Figure 5. Photograph of M1, M2, M3, and M4 color glasses.

M3 and M4 were achieved by depositing an additional layer of TiN (30 nm) on M1 and M2, respectively. M1 and M2 show shades of blue and green color glasses, respectively. It is demonstrated that tuning the thickness of the AlN changes the color of the film. M3 and M4 also show shades of green and yellow, respectively. Notable color deviation of samples from simulation may be due to thickness variation of the deposited layers from those in the simulation.

The transmittance and relative reflectance spectra of M1, M2, M3, and M4 color glasses within visible and NIR ranges are shown in Figure 6a,b, respectively. Maximum transmittance of more than 80% is achieved for all color glasses. The minimum transmittance peaks of M1, M2, M3, and M4 color glasses are 81% at 452 nm, 84% at 505 nm, 84% at 493 nm, and 86% at 553 nm, respectively. The relative reflectance of the samples also showed similar tendencies. The reflectance peak positions of M1, M2, and M3 color glasses are 26% at 449 nm, 24% at 502 nm, and 24% at 497 nm, respectively. The reflectance of M4 has peaks of 20 and 24% at 559 and 850 nm, respectively. In BIPV systems, it is desired that color glasses have high transmittance to ensure high efficiency. We have successfully demonstrated that color glasses with high transmittance of more than 80% can be achieved. For additional layers of TiN, reflectance of wavelengths above 500 nm are highly reflected as discussed in Figure 3a. Hence, it is confirmed in the M3 and M4 color glasses that transmittance is suppressed for incident beams with wavelengths more than 500 nm as compared to incident beams below 500 nm. The reflectance and transmittance of the color glasses can be tuned by the high refractive index material—AlN. The validation of the simulated results can be further enhanced by simulating with measured refractive index and thickness of films. Since AlN has similar refractive index with ITO, it is expected that color glasses can be fabricated solely with AlN and TiN without coating the glass substrates with ITO.

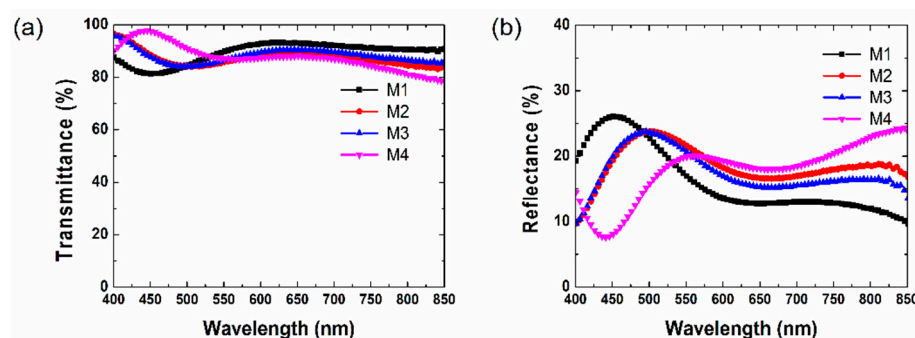


Figure 6. (a) Transmittance and (b) relative reflectance spectra of M1, M2, M3, and M4 color glasses.

4. Conclusions

We fabricated color glasses for BIPV systems using multilayer thin films composed of titanium nitride and aluminum nitride layers. The high refractive index AlN layer, combined with the low refractive index TiN layer, provided an effective multilayer structure for achieving desired colors with good transmittance. It was investigated that the multilayer structure and the thickness of the AlN and TiN layers can tune the color and transmittance of the film. Blue, green, and yellow color glasses were achieved with the ITO-coated glass/TiN/AlN multilayer structure by tuning the number and thickness of the layers. It is successfully demonstrated that color glasses with a high transmittance of more than 80% can be achieved. The proposed multilayer structure and the adopted sputtering technique allows cheap and desirable color glasses to be implemented in commercial BIPV systems and other photonic devices.

Author Contributions: Conceptualization, Y.C., J.-H.L., and A.G.; formal analysis, Y.C., J.-H.L., and A.G.; investigation, Y.C., J.-H.L., A.G., and H.-S.A.; methodology, S.L., H.-S.A., and A.G.; writing—original draft, A.G.; writing—review and editing, A.G., H.-S.A., Y.C., and J.-H.L. All authors have read and agreed to the published version of the manuscript.

Funding: This work was supported by basic science research program through the NRF funded by the ministry of Education(NRF-2018R1A6A1A03026005) and by the research fund of Hanbat National University in 2017.

Data Availability Statement: The data presented in this study are available on request from the corresponding authors.

Conflicts of Interest: The authors declare no conflict of interest.

References

1. Cerón, I.; Caamaño-Martín, E.; Neila, F.J. ‘State-of-the-art’ of building integrated photovoltaic products. *Renew. Energy* **2013**, *58*, 127–133. [CrossRef]
2. Shukla, A.K.; Sudhakar, K.; Baredar, P. Recent advancement in BIPV product technologies: A review. *Energy Build.* **2017**, *140*, 188–195. [CrossRef]
3. Wolf, M. Performance analysis of combined heating and photovoltaic power systems for residences. *Energy Convers.* **1976**, *16*, 79–90. [CrossRef]
4. Florschuetz, L.W. Extension of the Hottel-Whiller model to the analysis of combined photovoltaic/thermal flat plate collectors. *Sol. Energy* **1979**, *22*, 361–366. [CrossRef]
5. Kippelen, B.; Brédas, J.-L. Organic photovoltaics. *Energy Environ. Sci.* **2009**, *2*, 251–261. [CrossRef]
6. Nam, E.-H.; Lee, D.-H.; Kim, C.-G.; Namkung, H.-S.; Park, D.-K.; Woo, H.-S. Increasing the efficiency of a multilayer bulk heterojunction solar cell using water-soluble conjugated polymer as an electron injection layer. *J. Inf. Disp.* **2016**, *17*, 37–41. [CrossRef]
7. Amado, M.; Poggi, F. Solar Energy Integration in Urban Planning: GUUD Model. *Energy Procedia* **2014**, *50*, 277–284. [CrossRef]
8. Kazmerski, L.L. Photovoltaics: A review of cell and module technologies. *Renew. Sustain. Energy Rev.* **1997**, *1*, 71–170. [CrossRef]
9. Schüler, A.; Roecker, C.; Boudaden, J.; Oelhafen, P.; Scartezzini, J.-L. Potential of quarterwave interference stacks for colored thermal solar collectors. *Sol. Energy* **2005**, *79*, 122–130. [CrossRef]
10. Mertin, S.; Caër, V.H.-L.; Joly, M.; Mack, I.; Oelhafen, P.; Scartezzini, J.-L.; Schüler, A. Reactively sputtered coatings on architectural glazing for coloured active solar thermal façades. *Energy Build.* **2014**, *68*, 764–770. [CrossRef]
11. Guo, Y.; Shoyama, K.; Sato, W.; Nakamura, E. Polymer stabilization of lead (II) perovskite cubic nanocrystals for semitransparent solar cells. *Adv. Energy Mater.* **2016**, *6*, 1502317. [CrossRef]
12. BJ Power Co. Ltd. Solar Power System, Solar Modules. Available online: <https://bjpower.en.ec21.com/> (accessed on 14 August 2020).
13. SwissInso. SwissINSO–Technology. Available online: <https://www.swissinso.com/technology> (accessed on 12 August 2020).
14. Ahn, H.-S.; Gasonoo, A.; Jang, E.-J.; Kim, M.-H.; Lee, J.-H.; Choi, Y. Transition Metal Oxide Multi-Layer Color Glass for Building Integrated Photovoltaic System. *J. Inst. Korean Electr. Electron. Eng.* **2019**, *23*, 1128–1133.
15. Gasonoo, A.; Ahn, H.-S.; Kim, M.-H.; Lee, J.-H.; Choi, Y. Metal Oxide Multi-Layer Color Glass by Radio Frequency Magnetron Sputtering for Building Integrated Photovoltaic System. *J. Inst. Korean Electr. Electron. Eng.* **2018**, *22*, 1056–1061.
16. Stavenga, D.G. *Thin Film and Multilayer Optics Cause Structural Colors of Many Insects and Birds*; Elsevier BV: Amsterdam, The Netherlands, 2014; Volume 1, pp. 109–121.
17. Tien, P.K. Light Waves in Thin Films and Integrated Optics. *Appl. Opt.* **1971**, *10*, 2395–2413. [CrossRef] [PubMed]

18. Krasnov, A.N.; Kim, W.Y. Improved Human Factors of Electroluminescent Displays using Optical Interference Effect. *J. Inf. Disp.* **2003**, *4*, 7–12. [[CrossRef](#)]
19. Lam, W.-S.T. Optical Interference Coatings. Available online: <http://www.u.arizona.edu/~waisze/report.html/> (accessed on 25 February 2021).
20. Banerjee, A.; Dutta, G.S.; Ghosh, N. *Wave Optics: Basic Concepts and Contemporary Trends*; CRC Press: Boca Raton, FL, USA, 2015.
21. Hecht, E. *Optics*, 5th ed.; Addison-Wesley: Boston, MA, USA, 2016.
22. Kim, L.H.; Kim, K.; Park, S.; Jeong, Y.J.; Kim, H.; Chung, D.S.; Kim, S.H.; Park, C.E. Al₂O₃/TiO₂ Nanolaminate Thin Film Encapsulation for Organic Thin Film Transistors via Plasma-Enhanced Atomic Layer Deposition. *ACS Appl. Mater. Interfaces* **2014**, *6*, 6731–6738. [[CrossRef](#)]
23. Gasonoo, A.; Lee, J.-H.; Lim, Y.-J.; Lee, S.-H.; Choi, Y.; Lee, J.-H. Parylene C-AlN Multilayered Thin-Film Passivation for Organic Light-Emitting Diode Using a Single Deposition Chamber. *Electron. Mater. Lett.* **2020**, *16*, 466–472. [[CrossRef](#)]
24. Yang, Y.; Sun, X.; Chen, B.; Xu, C.; Chen, T.; Sun, C.; Tay, B.K.; Sun, Z. Refractive indices of textured indium tin oxide and zinc oxide thin films. *Thin Solid Film.* **2006**, *510*, 95–101. [[CrossRef](#)]
25. Nowicki, R.S. Properties of rf-sputtered Al₂O₃ films deposited by planar magnetron. *J. Vac. Sci. Technol.* **1977**, *14*, 127–133. [[CrossRef](#)]